Journal of Hazardous Materials 470 (2024) 134145

Contents lists available at ScienceDirect

Journal of Hazardous Materials

journal homepage: www.elsevier.com/locate/jhazmat

Oxidation of branched chain amino acids by HOCl: Kinetics and mechanism

Fruzsina Simon [b], István Fábián [a,b], Mária Szabó [a,b,*]

[a] Department of Inorganic and Analytical Chemistry, University of Debrecen, Debrecen, Hungary
[b] HUN-REN-UD Mechanisms of Complex Homogeneous and Heterogeneous Chemical, Reactions Research Group, University of Debrecen, Debrecen, Hungary

HIGHLIGHTS

- The products and the main intermediates have been identified.
- At high pH, the formation of *N*,*N*-dichloroamino acids does not occur.
- At pH~7, the reactions of monochloroamino acids with Cl_2O yield dichloroamino acid.
- Detailed mechanisms are postulated for the interpretation of the results.
- Nitriles as main products and chlorinated by-products have been identified.

GRAPHICAL ABSTRACT

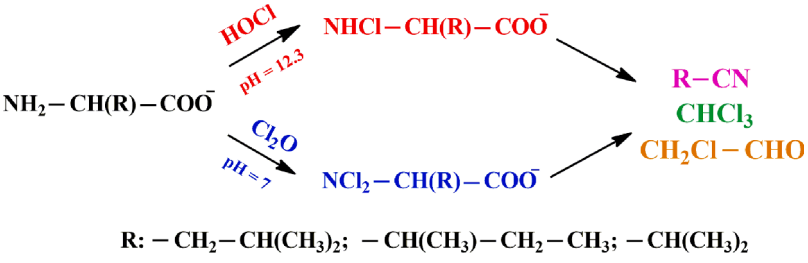

R: $-CH_2-CH(CH_3)_2$; $-CH(CH_3)-CH_2-CH_3$; $-CH(CH_3)_2$

ARTICLE INFO

Keywords:
Chlorination
Water treatment
N
N-dichloroamino acid
Halogenated byproduct
Kinetics and mechanism

ABSTRACT

The kinetics of the chlorination of leucine, isoleucine, and valine (BCAAs) was studied in excess HOCl by stopped-flow and spectrophotometric methods (25 °C, I = 1.0 M $NaClO_4$). The intermediates and products were identified and monitored by ^1H NMR spectroscopy. It was established that these reactions are fully analogous and proceed according to distinct mechanisms under alkaline and neutral conditions. At high pH, the formation and subsequent rate determining decomposition of *N*-monochloroamino acid control the process. The decomposition occurs via competing pH-independent and OH^--assisted reaction paths and the sequence of chlorination, dichlorination and decarboxylation steps leads to the formation of *N*-chloroimines and their carbanionic forms, which are in fast acid – base equilibria. The dechlorination of the carbanions yields nitriles as the main products. The hydration of the *N*-chloro imines produces chloramine and aldehydes which are involved in further oxidation reactions with HOCl. The formation of chloroform and chloroacetaldehyde was confirmed in each system. At pH 7.0, the *N*-chloro derivatives of BCAAs form immediately and are converted into the corresponding *N*,*N*-dichloro species within a few seconds after mixing the reactants. In this reaction, the reactive form of the oxidant is Cl_2O. The first-order decomposition of the dichloroamino acids occurs on stopped-flow timescale (k = 0.5 – 0.7 s^{-1}) and yields *N*-chloroimines which slowly decompose with a characteristic first-order rate constant on the order of a few times 10^{-5} s^{-1}. The main products are the corresponding nitriles that account for about 80% and 60% of the original amounts of amino acids under neutral and alkaline ($c_{\overline{OH}} = 5.00 \times 10^{-2}$ M) conditions, respectively. Aldehydes, carboxylic acids, chloroform and NCl_3 were also identified as by-products. The results unequivocally confirm that harmful chlorinated species may form from amino acids long after the chlorination step in water treatment technologies that deteriorates the quality of the finished water.
Environmental implication: In source waters, amino acids account for about 75% of the total dissolved nitrogen. Therefore, it is an essential issue how the reactions of these compounds with hypochlorite ion can be controlled to avoid the formation of toxic compounds. The compounds formed from BCAAs are considered to be harmful both under alkaline and neutral conditions (chloroacetaldehyde, chloroform, nitriles). However, some of the

* Corresponding author at: Department of Inorganic and Analytical Chemistry, University of Debrecen, Debrecen, Hungary.
E-mail address: szabo.maria@science.unideb.hu (M. Szabó).

https://doi.org/10.1016/j.jhazmat.2024.134145
Received 15 January 2024; Received in revised form 13 March 2024; Accepted 26 March 2024
Available online 28 March 2024

intermediates have extended lifetime in these systems and they may also react with other components of raw water during water treatment processes.

1. Introduction

Chlorine is widely used in the treatment and disinfection of drinking, waste, ballast and swimming pool waters [1–5]. The prevalence of this agent is due to its cost-effectiveness and high efficiency in microbial disinfection and inactivation of pathogens. During the chlorination process, chlorine gas is introduced into the treated water, where it rapidly converts into hypochlorous acid [6]. Alternatively, the use of sodium hypochlorite or hypochlorous acid solutions is also feasible. HOCl, ClO^-, Cl_2 and Cl_2O are always present in equilibria controlled by the pH and collectively referred to as hypochlorous acid (HOCl) in this study. Distinction between these forms is made only when required for the clarity of presentation. Typically, the active forms of the disinfectant are HOCl or Cl_2O, and the latter exists at low concentration in aqueous solution [7–9].

Free active chlorine species are very reactive in water. These compounds kill microorganisms, but also react with natural organic matter (NOM) and produce disinfection by-products (DBPs). Chlorinated DBPs mainly consist of trihalomethanes (THMs), halonitromethanes (HNMs), haloacetic acids (HAAs), haloacetonitriles (HANs), haloketones (HKs) etc., which have detrimental effects on human health [10,11]. Although the concentrations of nitrogen-containing DBPs (N-DBPs: HANs, HNMs etc.) are generally lower than those of carbonaceous DBPs (C-DBPs: THM, HAAs etc.), N-DBPs have received more attention in recent years due to their higher genotoxicity and cytotoxicity [12–14]. These compounds are classified as carcinogenic because they may induce severe protein-DNA damage, inhibit DNA self-healing and affect the life cycle of cells [15–17]. The main precursors of N-DBPs are ammonia and various dissolved organic nitrogen compounds (DON), such as amino acids, proteins, urea, pharmaceutical and personal care products (PPCPs) [18–20]. Some of the chlorinated species have a low odor and taste perception threshold and thus contribute to the decline of water quality [1,21,22]. This is a primary concern because the aesthetic properties predominantly determine the judgment of the consumer on water quality [23].

N-monochloroamino acids form in very fast pH dependent reactions when hypochlorous acid reacts with excess amino acids [24–26]. Such conditions are relevant mainly in biological systems [27]. In recent studies, we have shown that these compounds undergo spontaneous decomposition within a few hours at most [26,28–30]. In water treatment technologies, HOCl is typically in excess over the amino acids. While *N*-monochloroamino acids also form, subsequently they are oxidized fully or in part to further products depending on the actual conditions. Again, the duration of these processes is a few hours [31]. Since the distribution of drinking water via the water network system occurs on a considerably longer time scale, the consumers are more likely exposed to the decomposition and oxidation products of chloramines than to the primary chlorinated species. The possibility for long-term post-chlorination reactions is also feasible in the treatment of other types of water. Accordingly, meticulous kinetic and mechanistic studies are required to explore the transformation of *N*-chlorinated species and to identify the final products formed in these reactions. Recently, we have shown that the decomposition of *N*-monochloroamino acids is a multi-step process which includes the formation and further reactions of reactive intermediates. It was confirmed that the variation of the pH has profound effect on the decomposition kinetics, and the presence of alkyl substituents on the α-carbon atom significantly alters the mechanism [26,28–30]. The chlorination of glycine and α-alanine in HOCl excess features even larger diversity both in terms of kinetics and mechanism [32]. In both systems, the observations have been interpreted by the combination of two limiting mechanisms established under neutral and alkaline conditions where the active chlorinating agent is Cl_2O and HOCl, respectively. While the *N,N*-dichloroamino acids are key reactive intermediates at pH ~ 7, they do not form in alkaline solution where the decomposition of the *N*-monochloro species controls the overall process. The chlorination of the two simplest amino acids shows different features due to the presence of the α-methyl group in α-alanine.

Scully et al. have studied the reactions between various amino acids and HOCl and identified aldehydes, nitriles and *N*-chloroaldimines as DBPs at different Cl / N molar ratios in the pH 7.0 – 11.0 range. In these papers, general reaction schemes were proposed without studying the kinetics of the corresponding reactions in detail [33–36]. Recently, the chlorination of valine and leucine have been reported at 2.8 and 2.4 Cl / N molar ratios and limiting the pH to 7.5 and 7.0, respectively [31,37]. The proposed mechanisms postulate that HOCl is the reactive form of the chlorinating agent; the rate constants of the reaction between HOCl and the amino acids is on the order of $10^4\ M^{-1}s^{-1}$; the decomposition of the *N*-monochloroamino acids directly contributes to the formation of reactive intermediates under the applied conditions; and the half-life of the *N,N*-dichlorovaline and *N,N*-dichloroleucine is 23 and 13 min. These findings are in contrast to the results and expectations based on the relevant literature. Most importantly, they imply that the chlorination of the essential branched chain amino acids (BCAAs) proceeds via a significantly different mechanism than the chlorination of glycine and α-alanine [32].

In this study, we provide a detailed account on the chlorination of BCAAs. It is an intriguing issue whether the bulky alkyl substituents in α-position can significantly alter the chlorination kinetics and induce a mechanistic changeover in the formation of *N,N*-dichloroamino acids. In this context, it is worthwhile to mention the most significant difference between the decomposition of *N*-monochloro-α-alanine and that of *N*-chloro BCAAs. The decomposition of the former compound proceeds via different reaction paths and yields different products under neutral and alkaline conditions [29]. In contrast, *N*-chloro BCAAs also decompose in a pH dependent manner, but the same final products are formed regardless of the pH [30]. We wish to explore if the same feature manifests itself in the oxidation of BCAAs by excess HOCl.

2. Experimental

2.1. Chemicals

All reagents were of the highest available analytical grade quality and used without further purification. The following chemicals were purchased from different distributors as indicated in parenthesis: leucine, isoleucine, valine, isobutyronitrile, isovaleronitrile, 2-methylbutyronitrile, isobutyraldehyde, isovaleraldehyde, 2-methylbutyraldehyde, chloroacetaldehyde, potassium iodide (Sigma-Aldrich); chloroform (VWR). Chloride ion free sodium hypochlorite solutions were prepared, standardized, and stored as described earlier [38,39]. In general, the pH was adjusted by using perchloric acid and sodium hydroxide solutions. Na_2HPO_4, NaH_2PO_4 (Sigma-Aldrich) were used as buffers in the pH 6.0 – 8.0 region. Except for the NMR measurements, 1.0 M ionic strength was always set with $NaClO_4$ solution. This compound was prepared from $HClO_4$ (Sigma-Aldrich) and anhydrous sodium carbonate (Reanal) as described earlier [40]. The samples were prepared in doubly deionized and ultrafiltered water obtained from a Purelab Classic (ELGA) water purification system.

2.2. Methods

Spectrophotometric studies were performed with Hewlett-Packard 8543 and Agilent Technologies Cary 8454 diode array spectrophotometers. The possibility of photochemical interference caused by the spectrophotometer was excluded by using different illumination protocols in repeated kinetic runs [41]. The temperature of the cell was controlled by a built-in thermoelectric Peltier device in the instrument. Cuvettes with different light pathlengths were used as required by the absorbance of the reaction mixtures. In all cases, 1.0 M $NaClO_4$ was the reference at the corresponding pH which was adjusted by administering NaOH or buffers.

Rapid reactions were monitored with an Applied Photophysics SX18MV stopped-flow instrument using a photomultiplier tube (PMT) attached as the detector. The kinetic traces were collected using 10.0 mm or 2.00 mm optical pathlengths and were obtained as an average of at least 3 repetitive runs. The deadtime of the stopped-flow instrument – t_d = 1.51 ms – was determined by monitoring the reduction of 2,6-dichlorophenol-indophenol (DCPIP) with excess ascorbic acid under pseudo-first order conditions [42].

pH measurement and titrations were performed with a Metrohm 888 Titrando automatic titrator using a Metrohm 6.0262.100 combination glass electrode. The same instrument was used for measuring the pH in the neutral – slightly alkaline region and the readout of the pH meter was converted into pH = − log[H^+] [43]. Iodometric titrations were made by using a Metrohm 6.0451.100 combination platinum electrode.

NMR spectra were recorded on a Bruker DRX-400 MHz spectrometer. The unit is equipped with a VT-1000 temperature controller and a 5 mm *z* grad BBI head. The measurements were carried out in aqueous solution and the signal of water protons (4.8 ppm) was suppressed using a watergate pulse sequence (12.6 dB). This is not an entirely selective method, and the integrals of the signals around the watermark are usually not proportional to the number of protons in the corresponding chemical environment. During the measurements, a capillary containing DSS (4,4-dimethyl-4-silapentane-1-sulfonic acid) solution was placed in the NMR tube and used as an external standard to determine the chemical shift of ^{1}H NMR signals. Spectra were recorded applying 32 scans with an acquisition time of 1.366 s and a 90° pulse. In the time resolved NMR experiments, the instrument was shimmed with the reaction mixture and the first spectra could be recorded about 180 s after initiating the reaction.

The experimental results were evaluated using MestReNova and WinNMR programs. The data from spectrophotometric experiments were evaluated using OriginPro 9.1 and Microsoft Excel. OriginPro 9.1 was also used to fit the kinetic curves [44].

3. Results and discussion

3.1. Alkaline conditions

To obtain reliable results with the kinetic methods applied here, the concentration of amino acids typically was 5.00 × 10^{-4} M in the experiments. While amino acids are present at lower concentration levels in source waters, certain waste waters may contain considerably higher amounts of these compounds. The validity of the results under drinking water treatment conditions was confirmed in dedicated experiments (vide infra).

The oxidation of BCAAs by excess hypochlorous acid shows composite kinetic features. Upon mixing the reactants under alkaline conditions (c^-_{OH} = 5.00 × 10^{-2} M), rapid initial increase and subsequent relatively slow decay of the absorbance was observed. It is reasonable to assume that these changes correspond to the formation and further oxidation of *N*- monochloro-BCAAs, respectively. The first step can conveniently be studied at the absorbance maximum of these species (λ_{max} ~ 255 nm) [30]. Analogous spectral changes were obtained with the three amino acids and the general features are demonstrated by showing results only for the oxidation of leucine. The corresponding figures for the other two systems are provided as Supplementary Material. As shown in Fig. 1 and Fig. S1, the formation of the *N*-monochloro-BCAAs (*N*-chloroleucine: MCL, *N*-chloroisoleucine: MCI and *N*-chlorovaline: MCV) follows simple first-order kinetics in the excess of HOCl and the kinetic traces were fitted to Eq. (1).

$$A = A_0 e^{-k_{obs} t} + A_\infty \quad (1)$$

where k_{obs} is the pseudo-first-order rate constant; A, A_0 and A_∞ are the actual, the initial and the final absorbance, respectively.

The plots of the pseudo-first-order rate constants (k_{obs}) as a function of HOCl concentration (Fig. 2) are in excellent agreement with our earlier results at amino acid excess [25]. This confirms that the reaction is an overall second-order process (Eq. (2)) and side-reactions do not occur with HOCl on this time scale.

$$d[c_{MC}]/dt = k_f\, c_{HOCl}\, c_{AA} \quad (2)$$

MC: *N*-chloro amino acid; AA: amino acid.

The calculated second-order rate constants, k_f = 400 ± 8, 393 ± 7, and 361 ± 13 M^{-1} s^{-1}, are in excellent agreement with previously reported results for the formation of MCL, MCI, and MCV at amino acid excess under the same conditions (c^-_{OH} = 0.05 M): 414, 392 and 377 M^{-1} s^{-1}, respectively [25]. These results and the ^{1}H NMR spectra (Fig. 5 and Fig. S5) confirm the formation of monochlorinated derivatives in the fast initial phase of the reaction.

At longer reaction times, the absorbance monotonously decreases at the absorption maximum of OCl^- (λ_{max} = 292 nm) in each system (Fig. 3 and Fig. S2).

The concentration of the unreacted HOCl was determined from the absorbance of the spent reaction mixture and plotted against the initial HOCl concentration (Fig. 4). According to these plots, 1 mol leucine, isoleucine and valine reacts with 4.0, 5.1 and 4.8 moles of hypochlorous acid, respectively.

In the 290–320 nm wavelength range, the absorbance decay can be fitted to a simple first-order rate expression (Fig. S3). The first-order rate constants, k_{da} are independent of the HOCl concentration (Fig. S4). This strongly suggests that the *N*-monochloro amino acids do not react directly with HOCl. Instead, they undergo spontaneous rate determining decomposition into intermediates which react with hypochlorous acid in subsequent reaction steps.

Time resolved ^{1}H NMR spectra are shown in Fig. 5 and Fig. S5. In

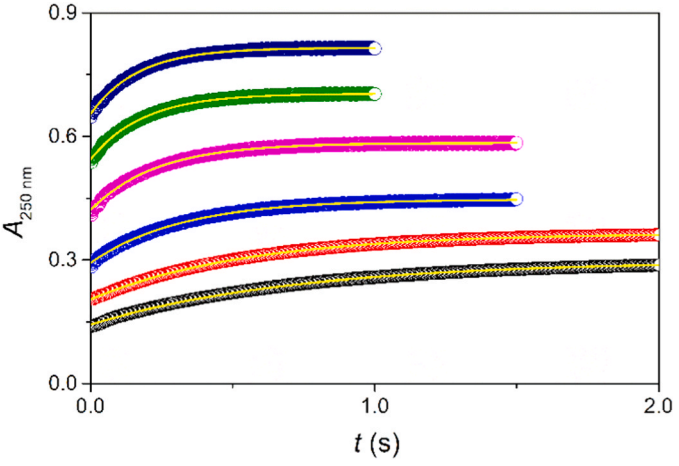

Fig. 1. Typical experimental (markers) and fitted (continuous lines) kinetic traces for the formation of *N*-chloroleucine (MCL) at excess HOCl under alkaline conditions. The traces were fitted to Eq. (1). c^0_{leu} = 5.00 × 10^{-4} M, c^0_{HOCl} = • 3.50 × 10^{-3} M, ● 5.00 × 10^{-3} M, ● 7.50 × 10^{-3} M, ● 1.00 × 10^{-2} M, ● 1.25 × 10^{-2} M, ● 1.50 × 10^{-2} M, c^-_{OH} = 5.00 × 10^{-2} M, I = 1.0 M ($NaClO_4$), T = 25.0 °C.

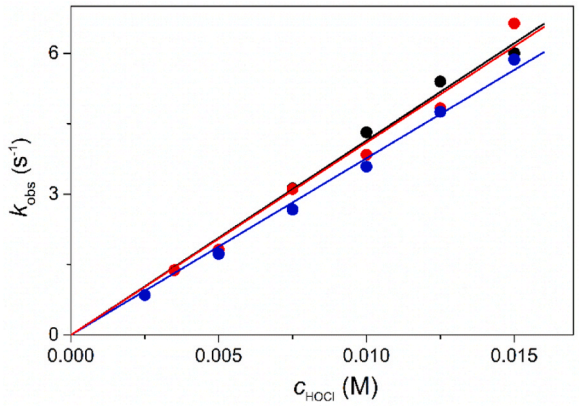

Fig. 2. The dependence of k_{obs} on the initial concentration of HOCl under alkaline conditions for the formation of MCL (black), MCI (red) and MCV (blue). The experimental data (marker) were fitted to a linear equation (solid line). $c^0_{aa} = 5.00 \times 10^{-4}$ M, $c_{\bar{OH}} = 5.00 \times 10^{-2}$ M, $I = 1.0$ M ($NaClO_4$), $T = 25.0$ °C.

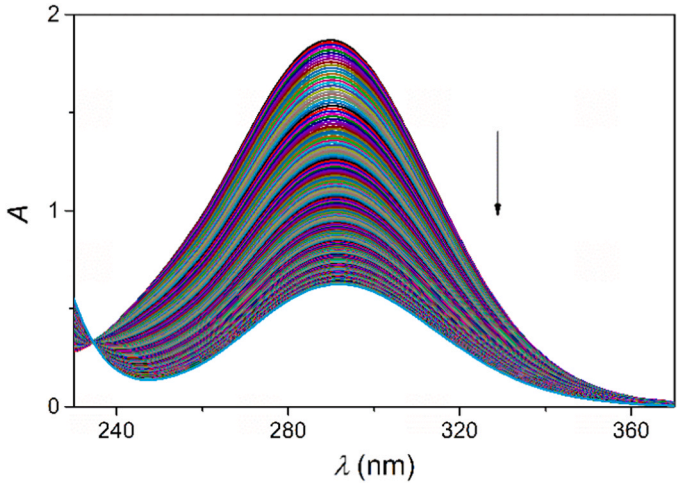

Fig. 3. Time resolved spectral changes recorded during the chlorination of leucine by excess HOCl under alkaline conditions. $c^0_{leu} = 5.00 \times 10^{-4}$ M, $c^0_{HOCl} = 2.50 \times 10^{-3}$ M, $c_{\bar{OH}} = 5.00 \times 10^{-2}$ M, $I = 1.0$ M ($NaClO_4$), $T = 25.0$ °C, $t = 160{,}00$ s, $\Delta t = 63$ s. The spectra are normalized to 1.00 cm light pass.

each case, the peaks of the first spectra (at ~ 180 s) are assigned to monochloroamino acids (MCL, MCI, MCV) in accordance with our previous results [30]. As expected on the basis of the above considerations, *N*,*N*-dichloro derivatives could not be identified in these spectra. Ultimately, the *N*-chloroamino acids are converted into the final products, which include isovaleronitrile (iVCN from leucine), 2-methylbutyronitrile (mbCN from isoleucine) and isobutyronitrile (iBCN from valine). The formation of these species was confirmed by comparing the spectra of the pure compounds and the spent reaction mixtures as shown in Fig. 6. In each system, the formation of chloroform ($CHCl_3$ 7.66 ppm) and chloroacetaldehyde (Cl-aca, 8.43 ppm) was also observed. These chlorination reactions were complete in several hours.

A close inspection of the spectra at the initial part of the reaction also reveals the formation of the corresponding chlorimines and aldehydes (leucine: isovaleraldehyde, ival; isoleucine: 2-methylbutyraldehyde, 2-mb-al; valine: isobutyraldehyde, ibal) as intermediates (Fig. S6). The ^{1}H NMR signals of these compounds are weak and disappear by the end of the reaction, but the characteristic peaks can clearly be identified.

It was confirmed in separate experiments that Cl-aca and $CHCl_3$ also form when the aldehydes are oxidized by excess HOCl (Fig. S7). This implies that the chlorination of the BCAAs always includes the oxidation of the covalent C – C bond between carbon atoms 2 and 3 of the aldehydes which are present as intermediates.

The intensity of the characteristic ^{1}H NMR peaks of the *N*-chloro BCAAs and the corresponding nitriles as a function of time can be fitted to a single exponential expression (Fig. 7 and Fig. S8). The NMR data for the two other products show similar time profiles but quantitative evaluation of the kinetic traces is not feasible because of the low intensity of the peaks. The calculated rate constants are in reasonable agreement with each other, and the results obtained from the spectrophotometric experiments considering that the ionic strength was not set in the NMR experiments (Table 1). According to our previous study, the decomposition of *N*-chloro BCAAs proceed parallel via pH-independent and OH^--assisted paths and $k_{da} = k + k_{OH}[OH^-]$ [30]. The rate constants obtained here and reported earlier at 0.05 M [OH^-] are also in excellent agreement.

The experimental results confirm that the chlorination of the three BCAAs by excess HOCl proceeds via fully analogous processes. The common kinetic model shown in Scheme 1 provides a plausible detailed interpretation of all observations. First, the *N*-monochloroamino acids form in relatively fast reaction steps. The decay of these species and the formation of the nitriles occur at the same rate, and the accumulation of intermediates in significant concentrations could not be detected in these systems. This implies that the rate determining decomposition of the *N*-chloro BCAAs controls the overall process. Via the pH independent path, their dechlorination and subsequent decarboxylation lead to the formation of imines that are the precursors of the corresponding *N*-chloro imines. The OH^- dependence of the decomposition is consistent with the formation of carbanions in an equilibrium step. These species lose chloride ion and convert into imino acids, which are *N*-chlorinated and undergo decarboxylation. This reaction sequence leads to the formation of the carbanionic form of the *N*-chloro imines produced via the other reaction path and these species are involved in fast acid-base equilibria. The transfer of the electron from the negatively charged carbon atom to chlorine atom within the carbanions leads to the departure of Cl^- and the formation of nitriles. The hydration of the *N*-chloro imines produces aldehydes that are converted into the final products in further chlorination steps by HOCl. Semiquantitative evaluation of the ^{1}H NMR spectra reveals that the estimated concentrations of nitriles, chloroacetaldehyde and chloroform correspond to about 60%, 16% and 9% of the original amounts of amino acids, respectively. While analogous products are formed in the three systems, the alkyl substituents affect differently the rates of the individual reaction steps and the actual product distributions. This is the reason why these amino acids consume somewhat different amounts of HOCl by the end of the reactions (cf. Fig. 4).

The mechanism postulates the direct chlorination of imines. The feasibility of this reaction was tested as follows. First, isobutyraldehyde and NH_4^+ were mixed in equimolar concentration ratio at pH ~ 5.0. After 10 min, this solution was reacted with fivefold excess of alkaline HOCl solution ($c_{\bar{OH}} = 5.00 \times 10^{-2}$ M). ^{1}H NMR spectra confirmed the formation of the corresponding *N*-chloroimine in a few minutes (Fig. S9).

While *N*-chloro acetamide is one of the final products in the chlorination of α-alanine under alkaline conditions[32], analogous compounds were not detected in the systems studied here. In all these reactions, an imine is formed as a reactive intermediate via the pH independent path. In the case of α-alanine, the hydration of ethaneimine yields 1-aminoethanol which undergoes chlorination to produce *N*-chloro-1-aminoethanol. Subsequent hydrolytic, dechlorination, hydration and chlorination steps lead to the formation of *N*-chloro acetamide. Most likely, the bulky alkyl groups of BCAAs inhibit the hydration of the corresponding imines and the chlorination of these intermediates becomes the dominant reaction path. Noteworthy that the OH^--assisted chlorination of α-alanine and BCAAs proceeds via the same reaction paths.

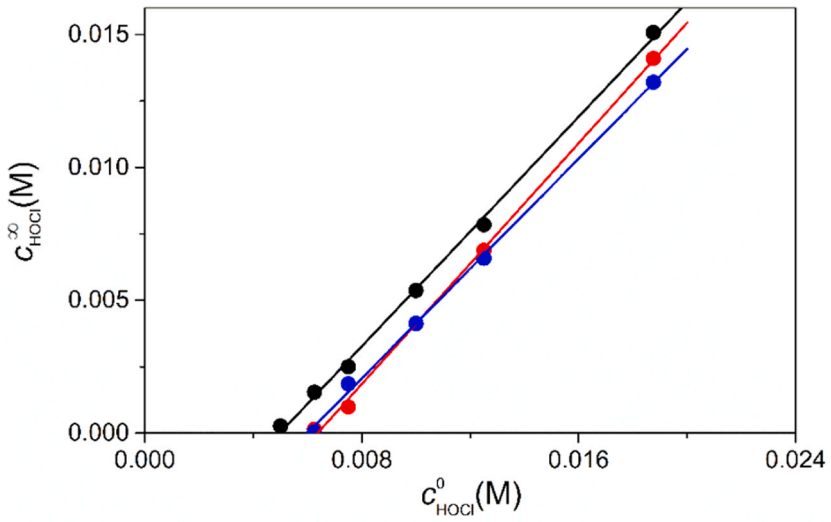

Fig. 4. The concentration of the unreacted hypochlorous acid at the end of the reaction as a function of the initial hypochlorous acid concentration under alkaline conditions: MCL (black), MCI (red) and MCV (blue). $c^0_{aa} = 5.00 \times 10^{-4}$ M, $c^-_{OH} = 5.00 \times 10^{-2}$ M, $I = 1.0$ M ($NaClO_4$), $T = 25.0$ °C.

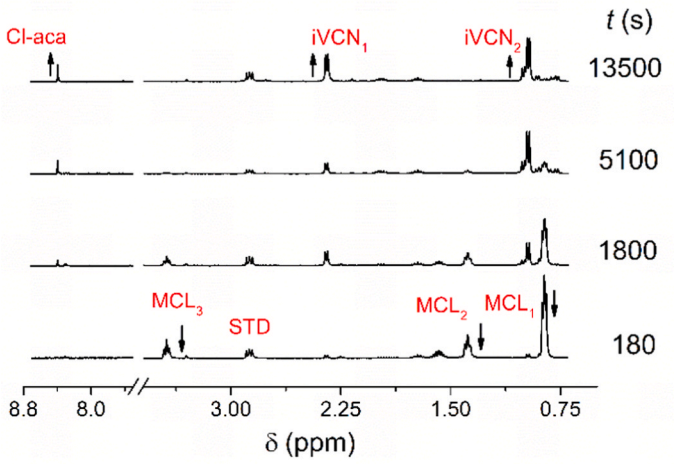

Fig. 5. Time resolved ^{1}H NMR spectra during the reaction of MCL with excess hypochlorous acid under alkaline conditions. $c^0_{leu} = 1.00 \times 10^{-2}$ M, $c^0_{HOCl} = 5.00 \times 10^{-2}$ M, $c^-_{OH} = 5.00 \times 10^{-2}$ M, $T = 25.0$ °C.

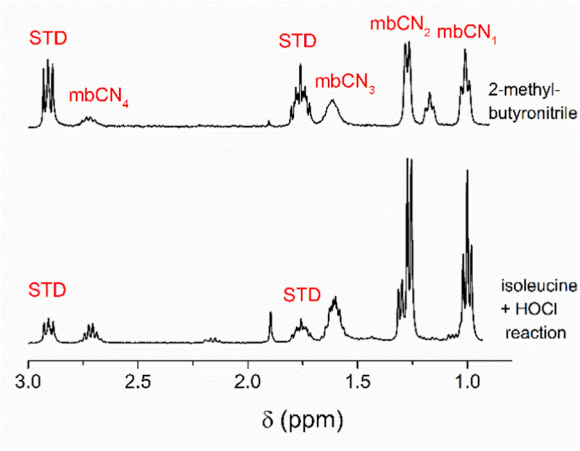

Fig. 6. The ^{1}H NMR spectra of a 1:5 reaction mixture of isoleucine and hypochlorous acid and the ^{1}H NMR spectra of 2-methylbutyronitrile under alkaline conditions. $c_{ileu} = 1.00 \times 10^{-2}$ M, $c_{HOCl} = 5.00 \times 10^{-2}$ M, $t = 86{,}400$ s, $c_{mbCN} = 5.00 \times 10^{-2}$ M, $c^-_{OH} = 5.00 \times 10^{-2}$ M, $T = 25.0$ °C.

3.2. Neutral conditions

Under neutral conditions, the analysis of the unreacted HOCl at the end of the reaction revealed that HOCl oxidizes leucine, isoleucine and valine according to 4.1: 1, 4.6: 1 and 4.2: 1 stoichiometry, respectively (Fig. S10). The fast initial phase of the reactions was studied by the stopped-flow method (Fig. 8 and Fig. S11). The kinetic traces exhibit composite patterns and feature an absorbance jump within the deadtime of the instrument. In accordance with our earlier results, this very fast step is due to the formation of mono-*N*-chloroamino acids [25]. The subsequent absorbance change corresponds to two partially overlapping first-order processes which complete in a few seconds. The kinetic curves recorded at 240 nm were fitted to Eq. (3).

$$A = A_1 e^{-k_{obs1} t} + A_2 e^{-k_{obs2} t} + A_\infty \quad (3)$$

These observations are consistent with the rapid chlorination of monochloroamino acids to *N*,*N*-dichloroamino acids (dichloroleucine: DCL, dichloroisoleucine: DCI and dichlorovaline: DCV, k_{obs1}), and the transformation of the latter species into a relatively stable intermediate (k_{obs2}) which slowly converts into the final products (vide infra).

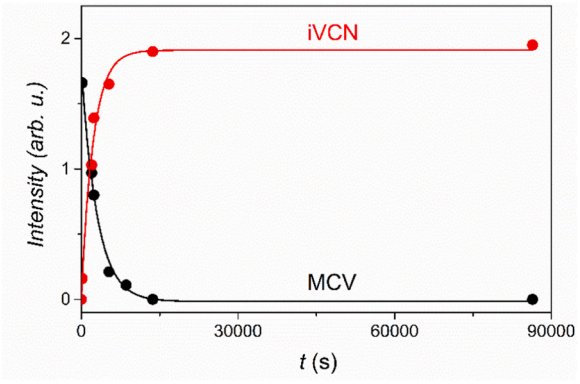

Fig. 7. The intensity of the characteristic ^{1}H NMR peaks of MCL (• 1.42 ppm) and iVCN (● 1.00 ppm) as a function of time. $c^0_{leu} = 1.00 \times 10^{-2}$ M, $c^0_{HOCl} = 5.00 \times 10^{-2}$ M, $c^-_{OH} = 5.00 \times 10^{-2}$ M, $T = 25.0$ °C.

Table 1
The first-order rate constants estimated on the basis of time resolved UV-Vis and ^{1}H NMR experiments and reported earlier[30] for the decomposition of *N*-chloro BCAAs.

N-chloro BCAA	$k_{da,\ UV\text{-}Vis} \times 10^4$ (s^{-1})	$k_{da,\ NMR} \times 10^4$ (s^{-1})	$k_{da,\ nitrile} \times 10^4$ (s^{-1})	$k_{da} \times 10^4$ (s^{-1}) [30]
MCL	2.65 ± 0.01	3.2 ± 0.5	4.5 ± 0.2	4.69
MCI	1.62 ± 0.01	2.0 ± 0.4	2.8 ± 0.5	2.47
MCV	1.60 ± 0.01	2.2 ± 0.1	2.0 ± 0.1	2.18

$c_{OH}^{-} = 0.05$ M, $T = 25.0$ °C.

The dependence of the pseudo-first-order rate constants on HOCl concentration was examined to establish the appropriate rate expressions for the two steps. Since one equivalent HOCl is consumed during the formation of *N*-chloro BCAAs, a corrected total concentration of HOCl was used in this procedure: $c_{HOCl}^{corr} = c_{HOCl}^{0} - c_{BCAA}^{0}$. As shown in Fig. 9, k_{obs1}/c_{HOCl}^{corr} is a linear function of c_{HOCl}^{corr} with zero intercept, i.e., the formation of the dichloro derivatives is second order in HOCl and overall a third order reaction. These results imply that dichlorine monoxide (Cl_2O) is the reactive form in the chlorination of *N*-chloro BCAAs under neutral condition. Cl_2O is in equilibrium with HOCl and always present at low concentration levels in aqueous solution [9]. While direct detection of this species is not feasible, numerous kinetic studies have served strong evidence that Cl_2O is a more efficient chlorinating agent than HOCl [8,32,45–51]. Our conclusion is corroborated by the earlier results.

The second order rate constant (k_{obs2}) does not depend on the HOCl concentration (Fig. S12), so the kinetic model detailed in Eq.s. (4) - (8) provides adequate interpretation of these observations.

$$HOCl \rightleftharpoons OCl^- + H^+ \quad K_a = \frac{[H^+][ClO^-]}{[HOCl]} \tag{4}$$

$$2HOCl \rightleftharpoons Cl_2O + H_2O \quad K_1 = \frac{[Cl_2O]}{[HOCl]^2} \tag{5}$$

$$AA + HOCl = MCAA + H_2O \text{ very fast} \tag{6}$$

$$MCAA + Cl_2O = DCAA + HOCl\ k_{Cl2O} \tag{7}$$

$$DCAA \rightarrow Int_1\ k_2 \tag{8}$$

Thus.

$$k_{obs1} = k_{Cl2O} K_1 \left(\frac{1}{1+\frac{K_a}{[H^+]}}\right)^2 (c_{HOCl}^{corr})^2 \text{ and } k_{obs2} = k_2.$$

The kinetic traces were fitted to this model by using a non-linear least squares algorithm assuming that reactions 4 and 5 are fast preequilibria and using p$K_a = 7.40$ for HOCl [39]. The estimated parameters together with relevant results for the chlorination of glycine and α-alanine are listed in Table 2. The k_{Cl2O} K_1 values obtained independently in these systems are in excellent agreement and the first-order decomposition of the *N*,*N*-dichloro derivatives proceeds at very similar rates.

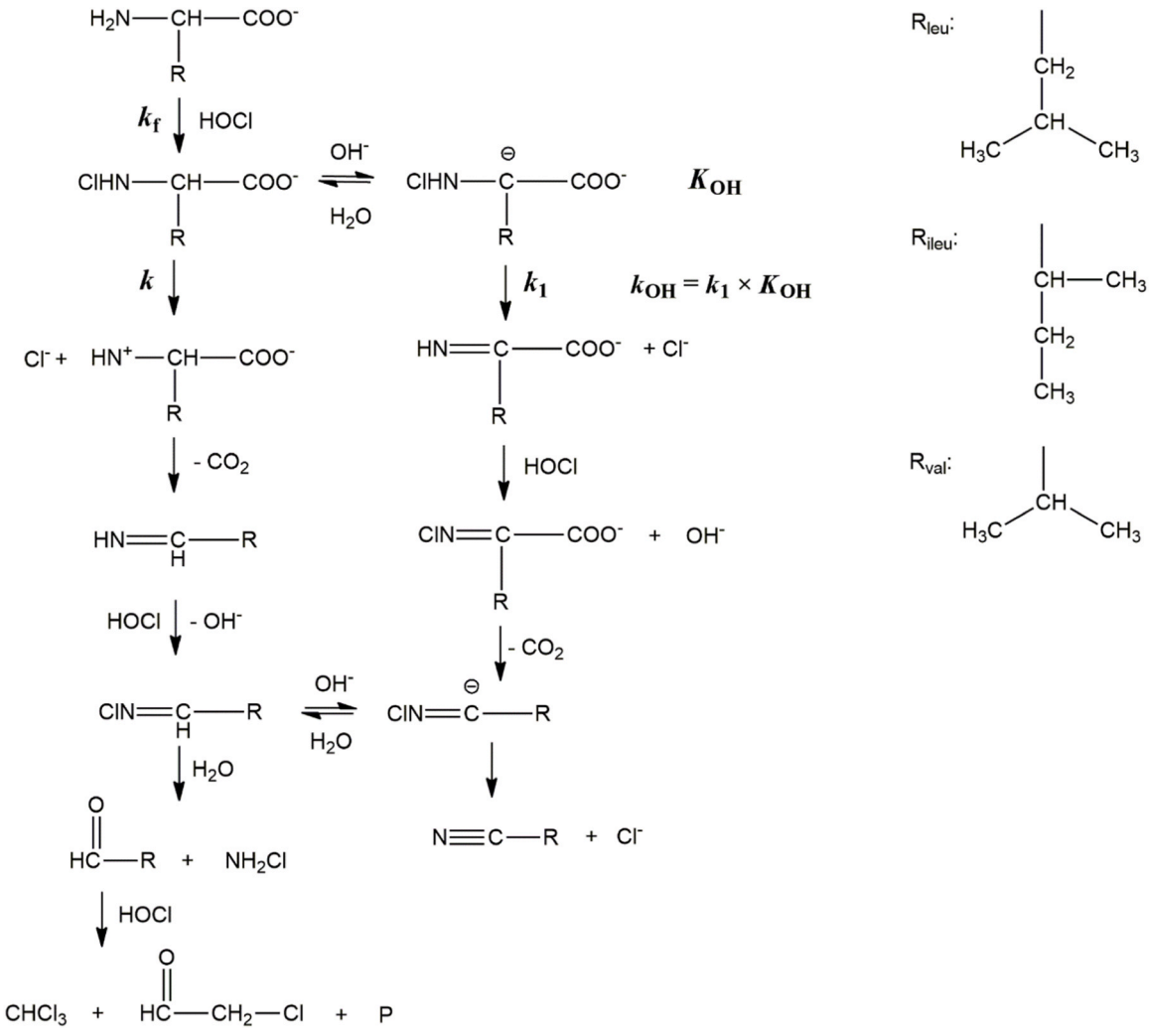

Scheme 1. The mechanism of the chlorination of branched-chain amino acids under alkaline conditions.

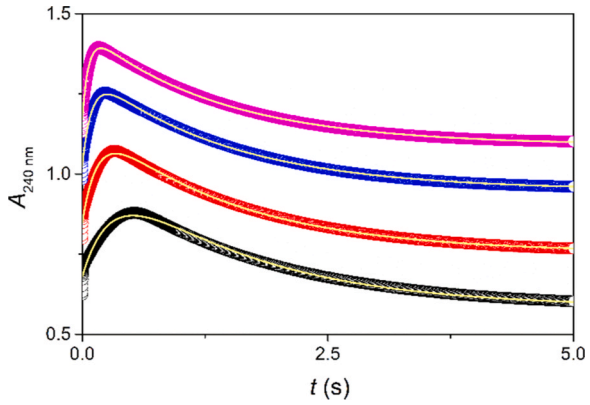

Fig. 8. Typical experimental (markers) and fitted (continuous lines) kinetic traces for the formation and decomposition of DCL at excess HOCl in neutral solution. The traces were fitted to Eq. (3). $c^0_{leu} = 5.00 \times 10^{-4}$ M, $c^0_{HOCl} =$ • 8.00×10^{-3} M, ● 1.05×10^{-2} M, ● 1.30×10^{-2} M, ● 1.55×10^{-2} M, I = 1.0 M ($NaClO_4$), pH = 6.92, T = 25.0 °C.

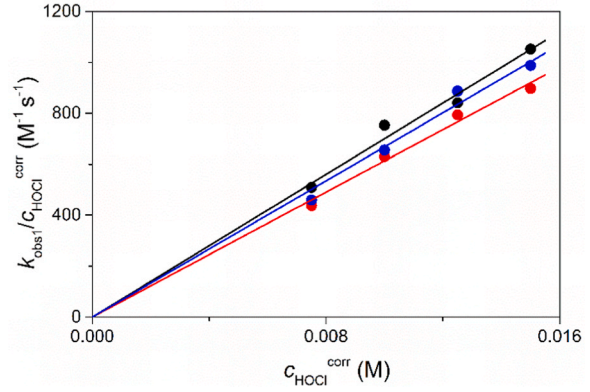

Fig. 9. The dependence of k_{obs1} on the corrected concentration of HOCl under neutral condition in the leucine (black), isoleucine (red) and valine (blue) – HOCl system. $c^0_{aa} = 5.00 \times 10^{-4}$ M, pH = 6.92, I = 1.0 M ($NaClO_4$), T = 25.0 °C.

Table 2
The k_{Cl2O} K_1 and the k_2 constants for the formation and decomposition of *N,N*-chloro BCAAs. T = 25.0 °C.

N,N-dichloro BCAA	k_{Cl2O} $K_1 \times 10^{-5}$ ($M^{-1}s^{-1}$)	k_2 (s^{-1})
DCL	1.22 ± 0.07	0.70 ± 0.01
DCI	1.10 ± 0.04	0.57 ± 0.01
DCV	1.29 ± 0.07	0.46 ± 0.01
glycine [32]	1.52	na
α-alanine [32]	1.19	0.29

The intermediate formed in this phase of the reaction is slowly converted into the final products over almost a day. The first ^{1}H NMR spectra recorded after mixing the reactants confirm that the noted intermediates are *N*-chloroimines, i.e., 1-chloroimino-3-methylbutane (1-Cl-3-mb), 1-chloroimino-2-methylbutane (1-Cl-2-mb) and 1-chloroimino-2-methylpropane (1-Cl-2-mp) formed from leucine, isoleucine and valine, respectively (Fig. 10 and Fig. S13). The main products in these reactions are nitriles that account for ~80% of the original amounts of the amino acids, but the corresponding aldehydes were also detected as minor components. Time resolved ^{1}H NMR experiments confirm that *N*-chloroimines decompose and the products form at about the same rates. Fitting the intensities of the selected peaks of *N*-chloroimines as a function of time to a simple exponential expression yields the following first-order rate constants (k_{dn}): (6.2 ± 0.5) 10^{-5} s^{-1}, (2.5 ± 0.4) 10^{-5} s^{-1}, (4.2 ± 0.6) 10^{-5} s^{-1} for 1-Cl-3-mb, 1-Cl-2-mb and 1-Cl-2-mp, respectively (Fig. S14).

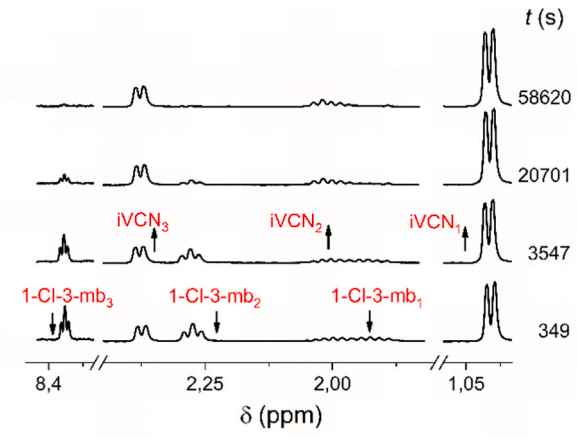

Fig. 10. Time resolved ^{1}H NMR spectra recorded in the chlorination of leucine under neutral conditions. $c^0_{leu} = 5.00 \times 10^{-3}$ M, $c^0_{HOCl} = 2.50 \times 10^{-2}$ M, pH = 6.92, T = 25.0 °C.

The formation of nitriles from the corresponding amino acids requires only two equivalents of HOCl. However, it was established experimentally that one amino acid consumes more than 4 equivalents of HOCl (cf. Fig. S10). This stoichiometry implies that higher oxidation state products and various chlorinated species also form in these systems. The detection of such compounds was not feasible in the reaction mixtures. This is not unexpected considering that the ^{1}H NMR peaks of these species may overlap with the peaks of the main products, may occur in the water suppressed region of the spectra or form at undetectable low concentration levels. Presumably, the additional products form via the aldehydes identified in these systems. In the reactions of isovaleraldehyde, 2-methybutyraldehyde and isobutyraldehyde with excess HOCl, the corresponding carboxylic acids were detected. In the case of isobutyraldehyde, some of the peaks could be assigned to Cl-aca and presumably to chloroform. The results strongly suggest that the same compounds also form during the chlorination of BCAAs.

Chloramine is also expected to form as a reactive byproduct, and it contributes to the consumption of hypochlorous acid. In excess HOCl, NH_2Cl is converted into NCl_3 that decomposes in subsequent reaction steps. Consequently, trichloramine is formed at low concentration level as a transient species and cannot be detected above pH 7.0. To corroborate these considerations, the chlorination reaction (isoleucine – HOCl 1:5) was triggered at pH 7.0, and the reaction mixture was made slightly acidic (pH ~ 6.0) after 240 s incubation time. These conditions stabilize NCl_3, and its formation could readily be confirmed by spectrophotometry at its characteristic absorbance band, λ_{max} = 220 nm (Fig. S15).

In the systematic kinetic and spectroscopic experiments discussed above, relatively high amino acid concentrations were used to obtain reliable and meaningful experimental data for the evaluation of the mechanism. To test the extendability of the results to drinking water treatment technologies, some of the experiments were performed at considerably lower concentration levels of amino acids ($c = 5.00 \times 10^{-5}$ M) that may occur in source waters [31]. In this case, the ^{1}H NMR spectra were recorded in reaction mixtures aged for 24 h ($c_{HOCl} = 2.50 \times 10^{-4}$ M, pH = 6.94). The sensitivity of the measurements was improved by using 1000 scans. Besides the corresponding nitriles, the formation of chloroacetaldehyde was confirmed in each system. In other words, the σ bond between carbon atoms 2 and 3 of the aldehyde derivates are prone for scission upon chlorination. It is noteworthy that the formation of chloroacetaldehyde was not observed during the chlorination of α-alanine. It was also confirmed in independent experiments that HOCl oxidizes acetaldehyde to acetic acid and chloro derivatives do not form in this reaction. In accordance with these findings, it is reasonable to

assume that the bulky alkyl moieties in the aldehydes promote the chlorination of carbon atom 2 and simultaneous scission of the carbon – carbon bond.

The ^{1}H NMR spectra lack the characteristic Cl-aca peak at higher amino acid concentrations. This can be the consequence of the transformation of this species into hemiacetal or further chlorinated species in subsequent reaction steps which are preferred by increasing the concentration. The corresponding products are expected to feature ^{1}H NMR peaks that overlap with the suppressed water signal, thus cannot be detected.

The mechanism proposed in Scheme 2 is fully consistent with the experimental results. In the rapid chlorination of the BCAAs, first the *N*, *N*-dichloro derivative is formed, which decomposes quickly. Accordingly, these compounds cannot be detected even in the first NMR spectra recorded approximately 180 s after mixing the reactants. The decomposition of the dichloro BCAAs yields *N*-chlorimines which are detected in the first spectra and the intensity of their peaks steadily decreases over the reaction. The dechlorination of these species directly produces the nitrile derivatives. *N*-chlorimines are also involved in hydration equilibria that lead to the formation of aldehydes and chloramine. It was confirmed in dedicated experiments that such equilibrium steps are operative in these systems. As demonstrated in the case of isoleucine, the reaction between 2-methylbutyraldehyde and monochloramine immediately produces *N*-chlorimine (1-chloro-imino-2-methylbutane) (Fig. 11). Irreversible reactions of the aldehydes with HOCl produce further oxidation products, such as carboxylic acids, chloroacetaldehyde, chloroform etc.

The results resolve the noted discrepancies in earlier literature (cf. Introduction). Thus, similarly to the chlorination of glycine and α-alanine, Cl_2O is the reactive form of the oxidant in the chlorination of the *N*-monochloro derivatives of BCAAs at pH 7.0. The corresponding *N*, *N*-dichloro derivatives readily transform into *N*-chlorimines and their half-life (a few seconds) is considerably shorter than proposed before. Finally, in contrast to earlier suggestions, the *N*-monochloro BCAAs are not directly involved in the formation of imines or the final products under neutral conditions.

4. Conclusions

The reactions of valine, leucine and isoleucine with excess HOCl are

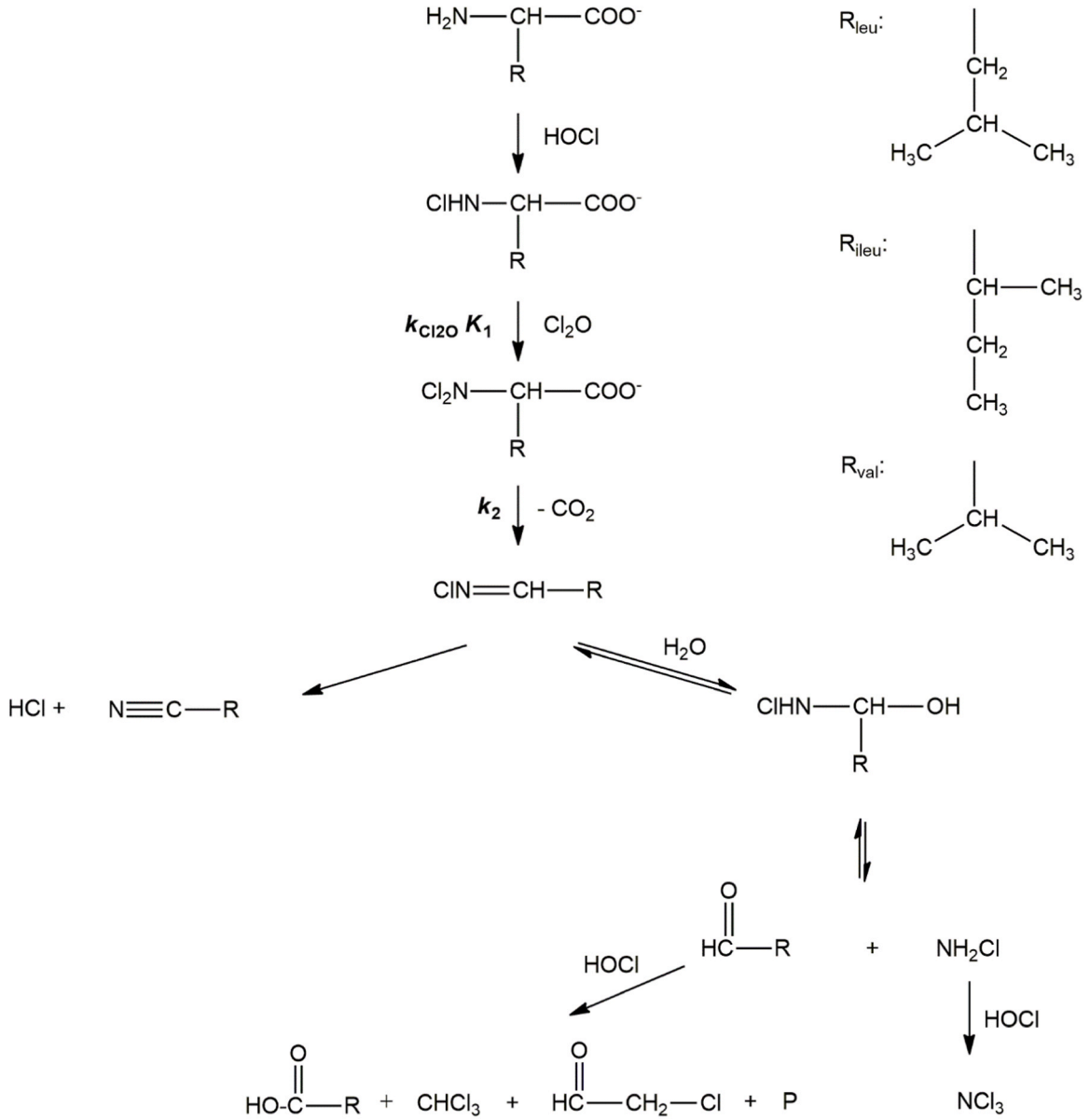

Scheme 2. The mechanism of the chlorination of branched-chain amino acids under neutral conditions.

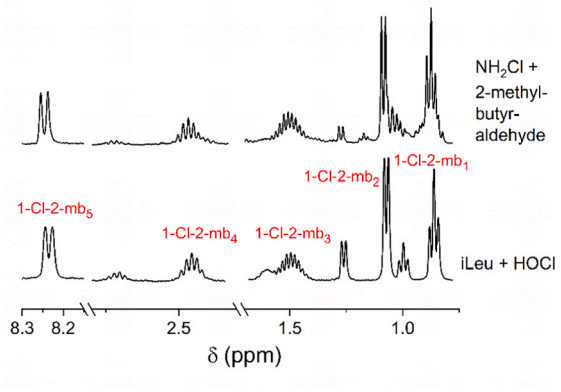

Fig. 11. Comparison of ^{1}H NMR spectra recorded for product identification under neutral conditions. $c_{ileu} = 1.00 \times 10^{-2}$ M, $c_{HOCl} = 5.00 \times 10^{-2}$ M, t = 272 s, $c_{aldehyde} = 1.00 \times 10^{-2}$ M, $c_{NH2Cl} = 1.00 \times 10^{-2}$ M, pH = 7.08, T = 25.0 °C.

fully analogous, but different mechanisms are operative under alkaline and neutral conditions. At high pH, the *N*-monochloroamino acids rapidly form and their rate determining slow decomposition controls the overall chlorination process. These reactions yield *N*-chloroimines and their carbanionic forms as intermediates which are in fast acid – base equilibria. These species convert into the final products via hydration and subsequent oxidation or dechlorination steps. At pH 7, imines are produced via the formation of *N*,*N*-dichloroamino acids. In further reaction steps, a larger variety of products forms than under alkaline conditions. These reactions show distinct features compared to the chlorination of glycine and α-alanine, i.e. full mineralization and the formation of *N*-chloro amides at high pH were not observed. Under neutral condition, the chlorination of BCAAs yields chloroacetaldehyde and chloroform as products while these compounds were not detected in the analogous reaction of α-alanine. The noted differences are attributed to the presence of the bulky alkyl groups in BCAAs. The results also confirm that earlier proposed mechanisms for these reactions do not provide accurate interpretation of the observations.

The results presented here unequivocally confirm that harmful chlorinated species may form from amino acids long after the chlorination step in water treatment technologies. A possibility for reducing the risk of these processes is the elimination of the precursor BCAAs by selective adsorption, pre-oxidative treatment of the raw water or using other dedicated methods. In addition, careful control of the chlorine dose is also recommended. In any case, the occurrence of potentially toxic disinfection byproducts needs to be carefully monitored on a case-by-case basis over an extended period of time during the use of chlorinated water.

CRediT authorship contribution statement

Dr Fruzsina Simon: Methodology, Formal analysis. **Dr István Fábián:** Writing – review & editing, Funding acquisition. **Mária Szabó:** Writing – original draft.

Declaration of Competing Interest

The authors declare the following financial interests/personal relationships which may be considered as potential competing interests: Istvan Fabian reports financial support was provided by National, Research, Development and Innovation Office.

Data Availability

Data will be made available on request.

Acknowledgements

This study was supported by the National Research, Development and Innovation Found of Hungary under grant number OTKA-139140 and by the University of Debrecen Program for Scientific Publication.

Appendix A. Supporting information

Supplementary data associated with this article can be found in the online version at doi:10.1016/j.jhazmat.2024.134145.

References

[1] White, G.C., 1992. Handbook of chlorination and alternative disinfectants. Van Nostrand Reinhold, New York.
[2] Lindmark, M., Cherukumilli, K., Crider, Y.S., Marcenac, P., Lozier, M., Voth-Gaeddert, L., Lantagne, D.S., Mihelcic, J.R., Zhang, Q.M., Just, C., Pickering, A.J., 2022. Passive in-line chlorination for drinking water disinfection: a critical review. Environ Sci Technol.
[3] Cheng, X., Wang, S., Huang, W., Wang, F., Fang, S., Ge, R., Zhang, Q., Zhang, L., Du, W., Fang, F., Feng, Q., Cao, J., Luo, J., 2022. Current status of hypochlorite technology on the wastewater treatment and sludge disposal: performance, principals and prospects. Sci Total Environ 803, 150085.
[4] Moreno-Andres, J., Peperzak, L., 2019. Operational and environmental factors affecting disinfection byproducts formation in ballast water treatment systems. Chemosphere 232, 496–505.
[5] Skibinski, B., Uhlig, S., Muller, P., Slavik, I., Uhl, W., 2019. Impact of different combinations of water treatment processes on the concentration of disinfection byproducts and their precursors in swimming pool water. Environ Sci Technol 53, 8115–8126.
[6] Crittenden, J.C., Trussel, R.R., Hand, D.W., Howe, K.J., Tchobanoglous, G., 2012. MWH's water treatment: principles and design edition 3. John Wiley & Sons, Hoboken, New Jersey.
[7] Deborde, M., von Gunten, U., 2008. Reactions of chlorine with inorganic and organic compounds during water treatment - kinetics and mechanisms: a critical review. Water Res 42, 13–51.
[8] Sivey, J.D., McCullough, C.E., Roberts, A.L., 2010. Chlorine Monoxide (Cl2O) and molecular chlorine (Cl-2) as active chlorinating agents in reaction of dimethenamid with aqueous free chlorine. Environ Sci Technol 44, 3357–3362.
[9] Roth, W.A., 1929. Zur Thermochemie des Chlors und der unterchlorigen Säure. Z Phys Chem 145A, 289–297.
[10] Hrudey, S.E., 2009. Chlorination disinfection by-products, public health risk tradeoffs and me. Water Res 43, 2057–2092.
[11] Kim, J., Chung, Y., Shin, D., Kim, M., Lee, Y., Lim, Y., Lee, D., 2003. Chlorination by-products in surface water treatment process. Desalination 151, 1–9.
[12] Hu, J.L., Chu, W.H., Sui, M.H., Xu, B., Gao, N.Y., Ding, S.K., 2018. Comparison of drinking water treatment processes combinations for the minimization of subsequent disinfection by-products formation during chlorination and chloramination. Chem Eng J 335, 352–361.
[13] Zhao, Y.L., Anichina, J., Lu, X.F., Bull, R.J., Krasner, S.W., Hrudey, S.E., Li, X.F., 2012. Occurrence and formation of chloro- and bromo-benzoquinones during drinking water disinfection. Water Res 46, 4351–4360.
[14] Richardson, S.D., Plewa, M.J., Wagner, E.D., Schoeny, R., DeMarini, D.M., 2007. Occurrence, genotoxicity, and carcinogenicity of regulated and emerging disinfection by-products in drinking water: a review and roadmap for research. Mutat Res-Rev Mutat Res 636, 178–242.
[15] Pero, R.W., Sheng, Y.Z., Olsson, A., Bryngelsson, C., LundPero, M., 1996. Hypochlorous acid N-chloramines are naturally produced DNA repair inhibitors. Carcinogenesis 17, 13–18.
[16] Kulcharyk, P.A., Heinecke, J.W., 2001. Hypochlorous acid produced by the myeloperoxidase system of human phagocytes induces covalent cross-links between DNA and protein. Biochemistry 40, 3648–3656.
[17] Hawkins, C.L., Pattison, D.I., Davies, M.J., 2002. Reaction of protein chloramines with DNA and nucleosides: evidence for the formation of radicals, protein-DNA cross-links and DNA fragmentation. Biochem J 365, 605–615.
[18] Ackerson, N.O.B., Killinger, A.H., Liberatore, H.K., Ternes, T.A., Plewa, M.J., Richardson, S.D., Duirk, S.E., 2019. Impact of chlorine exposure time on disinfection byproduct formation in the presence of iopamidol and natural organic matter during chloramination. J Environ Sci 78, 204–214.
[19] Bond, T., Huang, J., Templeton, M.R., Graham, N., 2011. Occurrence and control of nitrogenous disinfection by-products in drinking water - a review. Water Res 45, 4341–4354.
[20] Shen, R., Andrews, S.A., 2011. Demonstration of 20 pharmaceuticals and personal care products (PPCPs) as nitrosamine precursors during chloramine disinfection. Water Res 45, 944–952.
[21] Cai, L., Yu, S., Li, L., 2022. Formation of odorous aldehydes, nitriles and N-chloroaldimines from free and combined leucine during chloramination. Water Res 210, 117990.
[22] Cai, L.Y., Li, L., Yu, S.L., 2020. Formation of odorous aldehydes, nitriles and N-chloroaldimines from combined leucine in short oligopeptides during chlorination. Water Res 177.

[23] How, Z.T., Linge, K.L., Busetti, F., Joll, C.A., 2018. Formation of odorous and hazardous by-products from the chlorination of amino acids. Water Res 146, 10–18.
[24] Armesto, X.L., Canle L, M., García, M.V., Losada, M., Santaballa, J.A., 1994. N reactivity vs. O reactivity in aqueous chlorination. Int J Chem Kinet 26, 1135–1141.
[25] Szabó, M., Simon, F., Fábian, I., 2019. The formation of N-chloramines with proteinogenic amino acids. Water Res 165.
[26] Simon, F., Kiss, E., Szabó, M., Fábián, I., 2020. The chlorination of N-methyl amino acids with hypochlorous acid: kinetics and mechanisms. Chem Res Toxicol 33, 2189–2196.
[27] Pullar, J.M., Vissers, M.C.M., Winterbourn, C.C., 2000. Living with a killer: the effects of hypochlorous acid on mammalian cells. IUBMB Life 50, 259–266.
[28] Szabó, M., Baranyai, Z., Somsák, L., Fábián, I., 2015. Decomposition of N-chloroglycine in alkaline aqueous solution: kinetics and mechanism. Chem Res Toxicol 28, 1282–1291.
[29] Simon, F., Szabó, M., Fábián, I., 2019. pH controlled byproduct formation in aqueous decomposition of N-chloro-α-alanine. J Hazard Mater 362, 286–293.
[30] Szabó, M., Bíró, V., Simon, F., Fábian, I., 2020. The decomposition of N-chloro amino acids of essential branched-chain amino acids: kinetics and mechanism. J Hazard Mater 382.
[31] How, Z.T., Linge, K.L., Busetti, F., Joll, C.A., 2017. Chlorination of amino acids: reaction pathways and reaction rates. Environ Sci Technol 51, 4870–4876.
[32] Simon, F., Szabó, M., Fábián, I., 2023. The chlorination of glycine and α-alanine at excess HOCl: Kinetics and mechanism. J Hazard Mater 447, 130794.
[33] Conyers, B., Scully, F.E., 1993. N-chloroaldimines.3. Chlorination of phenylalanine in model solutions and in a waste-water. Environ Sci Technol 27, 261–266.
[34] McCormick, E.F., Conyers, B., Scully, F.E., 1993. N-chloroaldimines.2. Chlorination of valine in model solutions and in waste-water. Environ Sci Technol 27, 255–261.
[35] Nweke, A., Scully, F.E., 1989. Stable N-chloroaldimines and other products of the chlorination of isoleucine in model solutions and in waste-water. Environ Sci Technol 23, 989–994.
[36] Conyers, B., Walker, E., Scully, F.E., Marbury, G.D., 1993. N-chloroaldimines.4. Identification in a chlorinated municipal waste-water by gas-chromatography mass-spectrometry. Environ Sci Technol 27, 720–724.
[37] Cai, L., Li, L., Yu, S., 2020. Formation of odorous aldehydes, nitriles and N-chloroaldimines from combined leucine in short oligopeptides during chlorination. Water Res 177, 115803.
[38] Peintler, G., Nagypál, I., Epstein, I.R., 1990. Systematic design chemical oscillators - kinetics and mechanism of the reaction between chlorite ion and hypochlorous acid. J Phys Chem 94, 2954–2958.
[39] Adam, L.C., Fábian, I., Suzuki, K., Gordon, G., 1992. Hypochlorous acid decomposition in the pH 5-8 region. Inorg Chem 31, 3534–3541.
[40] Fábian, I., Gordon, G., 1991. Complex-formation reactions of the chlorite ion. Inorg Chem 30, 3785–3787.
[41] Fábian, I., Lente, G., 2010. Light-induced multistep redox reactions: the diode-array spectrophotometer as a photoreactor. Pure Appl Chem 82, 1957–1973.
[42] Tonomura, B., Nakatani, H., Ohnishi, M., Yamaguchiito, J., Hiromi, K., 1978. Test reactions for a stopped-flow apparatus - reduction of 2,6-dichlorophenolindophenol and potassium-ferricyanide by L-ascorbic-acidT. Anal Biochem 84, 370–383.
[43] Irving, H., Miles, M., Pettit, L., 1967. A study of some problems in determining the stoicheiometric proton dissociation constants of complexes by potentiometric titrations using a glass electrode. Anal Chim Acta 38, 475–488.
[44] O. 2018b, in, Microcal Software Inc., Northampton, MA, 2018.
[45] Thapliyal, P.C., Singh, K.P., Khanna, R.N., 1994. Chlorination of quinonoid compounds using dichlorine monoxide. Synth Commun 24, 1079–1083.
[46] Lau, S.S., Reber, K.P., Roberts, A.L., 2019. Aqueous chlorination kinetics of cyclic alkenes—Is HOCl the only chlorinating agent that matters? Environ Sci Technol 53, 11133–11141.
[47] Rose, M.R., Lau, S.S., Prasse, C., Sivey, J.D., 2020. Exotic electrophiles in chlorinated and chloraminated water: when conventional kinetic models and reaction pathways fall short. Environ Sci Technol Lett 7, 360–370.
[48] Sivey, J.D., Roberts, A.L., 2012. Assessing the reactivity of free chlorine constituents Cl2, Cl2O, and HOCl toward aromatic ethers. Environ Sci Technol 46, 2141–2147.
[49] Cai, M.-Q., Feng, L., Jiang, J., Qi, F., Zhang, L.-Q., 2013. Reaction kinetics and transformation of antipyrine chlorination with free chlorine. Water Res 47, 2830–2842.
[50] Cheng, H., Song, D., Chang, Y., Liu, H., Qu, J., 2015. Chlorination of tramadol: reaction kinetics, mechanism and genotoxicity evaluation. Chemosphere 141, 282–289.
[51] Beach, M.W., Margerum, D.W., 1990. Kinetics of oxidation of tetracyanonickelate (II) by chlorine monoxide, chlorine, and hypochlorous acid and kinetics of chlorine monoxide formation. Inorg Chem 29, 1225–1232.